On the influence of the thickness of the sediment moving layer in the definition of the bedload transport formula in Exner systems

Enrique D. Fernandez-Nieto, Carine Lucas, Tomas Morales de Luna, Stephane Cordier

On the influence of the thickness of the sediment moving layer in the definition of the bedload transport formula in Exner systems

E.D. Fernández-Nieto[a], C. Lucas[b], T. Morales de Luna[c,*], S. Cordier[b]

[a] *Dpto. Matemática Aplicada I. ETS Arquitectura - Universidad de Sevilla. Avda. Reina Mercedes N. 2. 41012-Sevilla, Spain*
[b] *MAPMO UMR CNRS 7349, Université d'Orléans, UFR Sciences, Bâtiment de mathématiques, B.P. 6759 - 45067 Orléans cedex 2, France*
[c] *Dpto. de Matemáticas. Universidad de Córdoba. Campus de Rabanales. 14071 Córdoba, Spain*

Abstract

In this paper we study Exner system and introduce a modified general definition for bedload transport flux. The new formulation has the advantage of taking into account the thickness of the sediment layer which avoids mass conservation problems in certain situations. Moreover, it reduces to a classical solid transport discharge formula in the case of quasi-uniform regime. And as a particular case we obtain a model that introduces saturated effects. We also present several numerical tests where we compare the proposed sediment transport formula with the classical formulation and we show the behaviour of the new model in different configurations.

1. Introduction

We are interested in the study of sediment transport in shallow water regimes. As it is said by Simons et al. in [1], sediment particles are transported by flow in one or a combination of ways: rolling or sliding on the bed (surface creep), jumping into the flow and then resting on the bed (saltation), and supported by the surrounding fluid during a significant part of its motion (suspension) (See Figure 1). There is no sharp line between saltation and suspension, and sediments may be transported partially by saltation and then suddenly be caught by the flow turbulence and transported in suspension. However, this distinction is important as it serves to delimit two methods of hydraulic transportation which follow different laws, *i.e.*, traction and suspension. This means that sediment transport occurs in two main modes: bedload and suspended load. Here we are going to focus on bedload transport and neglect suspension. The bed load is the part of the total load which is travelling immediately above the bed and is supported by intergranular collisions rather than fluid turbulence (see [2]). The suspended load, on the other hand, is the part of the load which is primarily supported by the fluid turbulence (c.f. [3]). Thus, bed load includes mainly sediment transport for coarse materials (saltation) or fine material on plane beds (saltation at low shear stresses and sheet flow at high shear stresses), although both types of transport can occur together and the limit is not always easy to define.
In the context of bedload transport, a mass conservation law also called Exner equation [4] is used to update the bed elevation. This equation is often coupled with the shallow water equations describing the overland flows (see for example [5, 6, 7, 8]). The complete system of PDE may be written in the form

$$\begin{cases} \partial_t h + \partial_x(hu) = 0 \\ \partial_t(hu) + \partial_x(hu^2 + gh^2/2) = -gh\partial_x(z_b + z_r) \\ \partial_t z_b + \partial_x \widehat{q_b} = 0 \end{cases} \tag{1}$$

where h is the water depth, u is the flow velocity, and z_b is the sediment layer that moves with the fluid. This sediment layer is supposed to stay on a non-erodible fixed layer of thickness z_r which is

*Corresponding author
Email addresses: edofer@us.es (E.D. Fernández-Nieto), carine.lucas@univ-orleans.fr (C. Lucas), tomas.morales@uco.es (T. Morales de Luna), stephane.cordier@math.cnrs.fr (S. Cordier)

Figure 1: Transport of particles by a flow

usually called the bedrock layer (see Figure 2). The sediment layer is usually assumed to be a porous layer with porosity φ. $\widehat{q_b}$ is the volumetric bedload sediment transport rate per unit time and width, described by some empirical law, and g is the acceleration due to gravity. The definition of $\widehat{q_b}$ includes the division by $(1-\varphi)$. The conservative variable hu is also called water discharge and noted by q.
Most classical models for sediment transport only consider a sediment layer that is transported by the fluid, including sometimes a bedrock layer z_r which is not modified by the fluid. One could assume that the sediment layer can be decomposed in two layers: a layer that moves due to the action of the river, whose thickness is denoted by z_m, and a layer composed by sediments that are not moving but are susceptible to move and denoted by z_f. In other words, particles within the layer z_f can be eroded and transferred to the moving layer z_m and particles moving within the layer z_m can stop and be deposed on the layer z_f. In general, we will have the relation

$$z_b = z_m + z_f. \tag{2}$$

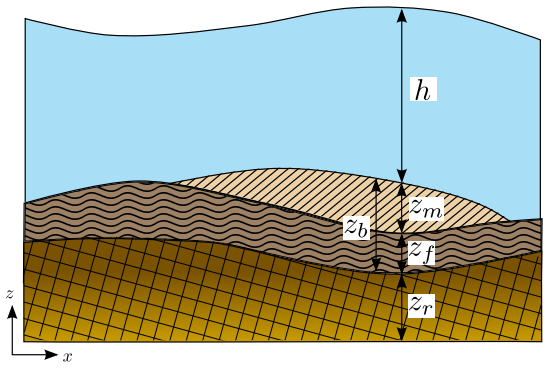

Figure 2: Sketch of shallow water over an erodible bed.

Despite the strong simplification hypotheses used in the derivation of the model and the lack of some good mathematical properties of the PDE system obtained (there is neither a momentum equation for the sediment layer nor an entropy pair) the approach of the bedload transport by means of an empirical solid transport discharge formula is widely spread for practical purposes: see for example [9], [10], [11], [4], [12].
In general, the solid transport discharge may depend on all the unknowns $\widehat{q_b} = \widehat{q_b}(h, hu, z_b, z_f)$ but classical formulae for this bedload transport only depend on the hydrodynamical variables h and u. With the purpose to distinguish whether solid transport discharge depends only on the hydrodynamical variables or on all the variables we use the following notation,

$$\widehat{q_b} = \begin{cases} q_b \equiv q_b(h, hu), \\ \widetilde{q_b} \equiv \widetilde{q_b}(h, hu, z_b, z_f). \end{cases}$$

Many different expressions of the solid transport discharge have been proposed in the literature. The formula proposed by Grass in [9] is among the simpler ones:

$$q_b(h, hu) = \frac{A}{1-\varphi} \left| \frac{hu}{h} \right|^{m-1} \frac{hu}{h} = \frac{A}{1-\varphi} |u|^{m-1} u,$$

where A is the constant of interaction between the fluid and the sediment layer and m is a parameter which is usually set to $m = 3$.
In practice, estimations of bedload transport rate are mainly based on the bottom shear stress τ_b, *i.e.* the force of water acting on the bed during its routing. The bottom shear stress is given as

$$\tau_b = \rho g h S_{\mathrm{f}},$$

where ρ is the water density and S_{f} is the friction term that can be quantified by different empirical laws such as the Darcy-Weisbach or Manning formulae

- Darcy-Weisbach:

$$S_{\mathrm{f}} = \frac{f u|u|}{8gh},$$

  where f is the Darcy-Weisbach's coefficient.

- Manning:

$$S_{\mathrm{f}} = \frac{n^2 u|u|}{h^{4/3}},$$

  where n is the Manning's coefficient.

The bottom shear stress is usually used in dimensionless form, noted τ_b^*, which is also called Shields parameter. It is defined as the ratio between drag forces and the submerged weight by

$$\tau_b^* = \frac{|\tau_b|}{(\rho_{\mathrm{s}} - \rho) g d_{\mathrm{s}}}, \tag{3}$$

where ρ_{s} is the sediment density and d_{s} is the diameter of sediment. The main hypothesis is that τ_b^* must exceed a threshold value τ_{cr}^* in order to initiate motion. The threshold value τ_{cr}^* depends on the physical properties of the sediment and is usually computed experimentally. One of the first works on this topic was done by Shields [13] in which τ_{cr}^* is determined in relation with the boundary Reynolds number.
The bedload transport rate may be represented as a function of τ_b^* via a non-dimensional function q_b^* by

$$q_b = q_b^*(\tau_b^*) \frac{\mathrm{sgn}(\tau_b)}{1-\varphi} Q. \tag{4}$$

where:

- for viscous laminar flows

$$Q = \frac{(\rho_s - \rho) g d_s^3}{\mu}, \tag{5}$$

  where μ is the dynamic viscosity. In [14] Charru et al. proposed the solid transport formula defined by

$$q_b^*(\tau_b^*) = \frac{0.85}{18} \tau_b^* (\tau_b^* - \tau_{cr}^*)_+.$$

  The value of τ_{cr}^* is of order of 0.1 for viscous laminar flows. Concretely, Charru et al. consider $\tau_{cr}^* = 0.12$.

- For turbulent flows we have

$$Q = \sqrt{\left(\frac{\rho_s}{\rho} - 1\right) g d_s^3}. \tag{6}$$

The following expressions have been often applied [10, 15, 12]:

$$\text{Meyer-Peter \& Müller (1948): } q_b^*(\tau_b^*) = 8(\tau_b^* - \tau_{cr}^*)_+^{3/2} \tag{7}$$

$$\text{Fernández Luque \& Van Beek (1976): } q_b^*(\tau_b^*) = 5.7(\tau_b^* - \tau_{cr}^*)_+^{3/2} \tag{8}$$

$$\text{Nielsen (1992): } q_b^*(\tau_b^*) = 12\sqrt{\tau_b^*}(\tau_b^* - \tau_{cr}^*)_+ \tag{9}$$

$$\text{Ribberink (1998): } q_b^*(\tau_b^*) = 11(\tau_b^* - \tau_{cr}^*)_+^{1.65} \tag{10}$$

In this case a characteristic value of τ_{cr}^* is 0.047.

Note that these classical bedload transport formulae can be written under the unified form

$$q_b(h, hu) = \frac{c}{1-\varphi} (\tau_b^*)^{m_1} (\tau_b^* - \tau_{cr}^*)_+^{m_2} \mathrm{sgn}(\tau_b) Q, \tag{11}$$

where $c > 0$, $m_1 \geq 0$ and $m_2 \geq 1$ are given constants. Q is defined by (5) for viscous laminar flows and by (6) for turbulent flows.
But given that classical formulae for solid transport flux only depend on the hydrodynamical variables, they do not take into account the thickness of the sediment layer. As a consequence the mass conservation law for the sediment layer may fail. For instance, let us suppose a situation like the one described in Figure 3, where the sediment layer is only present in the interior of the domain.

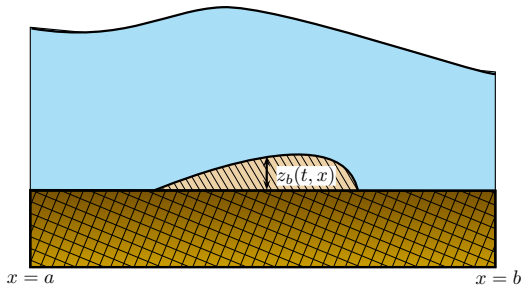

Figure 3: Sediment layer isolated in the interior of the domain

For instance, assume that we consider Meyer-Peter & Müller formula (7) and suppose that no sediment comes in or out of the domain through the boundaries during the time interval $[0, T]$. By integrating the third equation of (1) over $[0, T] \times [a, b]$, we obtain

$$\int_a^b (z_b)|_{t=T} dx - \int_a^b (z_b)|_{t=0} dx = -\int_0^T (\widehat{q_b}|_{x=b} - \widehat{q_b}|_{x=a})\, dt. \tag{12}$$

Let us suppose that the solid flux $\widehat{q_b}$ does not take into account the sediment layer thickness and only depends on the variables h and hu, *i.e.* $\widehat{q_b} = q_b$. Assume a velocity high enough in order to have $\tau_b^*(h, hu) > \tau_{cr}^*$ in (7) so that q_b is non-zero, and that h and hu are not equal at the boundaries $x = a$ and $x = b$. Then we will have $q_b|_{x=a} \neq q_b|_{x=b}$ and non-zero. Thus, in a situation like the one described in Figure 3 the right hand side in (12) may be non zero. This means that eventually the initial sediment mass is modified by an artificial flux at the boundary so that mass is not preserved.

In this paper we focus on the definition of the solid transport discharge $\widehat{q_b}$ in terms of the sediment thickness z_b. First, in Section 2 we review some of the results presented in the bibliography on the definition of the solid transport discharge $\widehat{q_b}$ in terms of z_b, erosion and deposition terms. In Section 3 we propose a new general formulation of the solid transport discharge. The proposed formula depends

on the moving sediment layer and the corresponding continuity equation preserves the sediment mass. Moreover, it reduces to a classical solid transport discharge formula in the case of quasi-uniform regime. In Subsection 3.2 we see that as a particular case of the proposed model we can obtain another one which is considered in the literature (see for example [16], [17], [18]) to introduce saturated effects in a classical model. In Section 4 we study the influence of the variable z_b on the eigenvalues of Exner system. First we show that Exner system is hyperbolic at least for physical situations. Second, we study the influence on the characterization of the sign of the eigenvalues of Exner system in terms of the hydraulic regime. In Section 5 we describe briefly the numerical approach for the simulation of the model by finite volume methods and we present some numerical results. Concretely, in Subsection 5.2 we compare the new sediment transport model introduced here with the classical formulation and we show the behaviour of the new model in different configurations.

2. On the definition of the solid transport discharge

We are interested here in the study of the evolution of the sediment layer at the bottom. In the evolution of the sediment layer z_b we can distinguish two different zones: a first layer that is moving due to the action of the fluid, z_m, and a second layer which is fixed, z_f, but consists of particles that could be entrained into movement within the moving layer z_m. Note that the thickness of the moving sediment layer is usually very small, of the order of one or two diameters of grains (see [19] and [20]). The total height of the sediment layer that can be affected by the fluid is denoted by $z_b = z_m + z_f$. The moving sediment layer is usually modeled as a whole by a continuity equation

$$\partial_t z_b + \partial_x \widehat{q_b} = 0, \tag{13}$$

where $\widehat{q_b} = \widetilde{q_b}(h, hu, z_b, z_f)$ is the solid transport discharge.

2.1. Dependence of the transport discharge on z_m

Following the structure of a continuity equation, the solid discharge can be written in the form

$$\widehat{q_b} = z_m v_b, \quad \text{(recall that } z_m = z_b - z_f, \text{ see equation (2))}, \tag{14}$$

where v_b is the bedload velocity. The problem is to find how to close the system by defining v_b. In fact, classical formulae define directly $\widehat{q_b}$ and not v_b (see equations (4)–(10)) and the dependence on z_m is not obvious due to several assumptions and simplifications.

The work by Fowler et al. in [19] (see also [21]) can be seen as a particular case of this idea of defining $\widehat{q_b}$ in the form (14). They propose a modified Meyer-Peter & Müller model which depends on the thickness of the sediment layer. This approach can be easily extended to any other classical bedload discharge. Suppose that $q_b(h, hu)$ is given by some classical empirical formula. Then, define

$$\widehat{q_b}(h, hu, z_b, z_f) = \widetilde{q_b}(h, hu, z_m) = \frac{z_m}{\bar{z}} q_b(h, hu)$$

where, $\bar{z}$ is a parameter of the model related to the mean value of the thickness of the sediment layer. We may replace (1) by

$$\begin{cases} \partial_t h + \partial_x(hu) = 0 \\ \partial_t(hu) + \partial_x(hu^2 + gh^2/2) = -gh\partial_x(z_b + z_r) \\ \partial_t z_b + \partial_x \widetilde{q_b} = 0. \end{cases} \tag{15}$$

In other words, we are considering a solid transport discharge in the form

$$\widetilde{q_b} = z_m v_b$$

with

$$v_b = \frac{q_b(h, hu)}{\bar{z}}.$$

These definitions of the bedload velocity and the solid transport discharge grant that if the thickness of the moving sediment layer vanishes then the solid transport discharge is equal to zero.

We will retake the idea of defining solid transport flux in the form (14) in Section 3.

2.2. Transport discharge in terms of erosion and deposition rates

In an erosion-deposition model (see for example [14], [22]), when sediment particles that are in the fixed bed are entrained into movement, they are considered to be part of the moving layer z_m. On the contrary, if the particles stop moving they are considered as part of the fixed layer z_f.
Let us denote by $\dot{z}_e$ the erosion rate and by $\dot{z}_d$ the deposition rate. In this situation, instead of the simple continuity equation (13), we may consider a more complex model which takes into account the transfer of particles between the fixed erodible layer z_f and the moving layer z_m. Then (1) can be generalized as

$$\begin{cases} \partial_t h + \partial_x(hu) = 0 \\ \partial_t(hu) + \partial_x(hu^2 + gh^2/2) = -gh\partial_x(z_b + z_r) \\ \partial_t z_m + \partial_x \widehat{q_b} = \dot{z}_e - \dot{z}_d, \\ \partial_t z_f = -\dot{z}_e + \dot{z}_d. \end{cases} \tag{16}$$

As we have $z_b = z_f + z_m$, by adding up the last two equations in (16) we recover (13). Let us remark that Charru et al. (see [14], [23], [22]) describe this model in terms of n instead of z_m, where n is the number of particles per unit time and unit bed area. These two quantities can be related together in terms of the diameter of the particles d_s and the porosity in the moving layer ψ: $nd_s^3 = (1-\psi)z_m$. For the sake of simplicity we consider $\psi = \varphi$, where φ can be seen as an averaged value of the porosity in the sediment layer. Anyway, recall that the moving layer is very small, then we can set φ as the porosity of the fixed sediment layer.
Now we specify the terms of the right hand side of system (16), that is, the erosion and deposition rate terms.

Deposition rate
In the literature we can find different definitions of the deposition rate $\dot{z}_d$, see for example [22], [17], [24]. We can write them under the uniform structure

$$\dot{z}_d = K_d V \frac{z_m}{d_s}, \tag{17}$$

where K_d is the deposition constant, V is the characteristic velocity, that we can define as

$$V = \frac{Q}{d_s}, \tag{18}$$

being Q the characteristic discharge. Q is defined by (5) for the case of laminar flows or by (6) for the case of turbulent flows. Let us remark that for viscous laminar flows, it is usual to consider $V = U_s$ the settling velocity. But, for the sake of simplicity, authors (see for example [22]) replace it by the Stokes velocity

$$U_s = \frac{(\rho_s - \rho)g d_s^2}{18\mu}. \tag{19}$$

Note that except the constant value 18 of the denominator – which can be introduced in the constant K_d of (17)– for the case of viscous laminar flows, the definition of V (18) coincides with the Stokes velocity definition (19).

Erosion rate.
If erosion is possible (*i.e.* $z_f > 0$), the erosion rate can be related to the shear stress, through the relation:

$$\dot{z}_e = K_e \frac{V}{(1-\varphi)}(\tau_b^* - \tau_{cr}^*)_+, \tag{20}$$

where K_e is the erosion constant and V is the characteristic velocity defined by (18).
In the following, we assume that z_f does not vanish.

Remark 2.1. *In [19], the erosion and deposition rates are defined in a different way, in terms of $\bar{z}$, $\bar{z}$ being a parameter of the model related to the mean value of the thickness of the sediment layer. It can be written under the following structure,*

$$\dot{z}_e - \dot{z}_d = K\frac{\bar{V}}{(1-\varphi)}(\tau_b^* - \tau_{cr}^*)_+^{3/2}\left(1-\frac{z_m}{\bar{z}}\right)_+, \quad \textit{with} \quad \bar{V} = \sqrt{g d_s}\frac{d_s}{\bar{z}}\frac{\sqrt{\rho_s-\rho}}{\sqrt{\rho}},$$

being K a constant parameter.

3. General formulation for the solid transport discharge

The solid transport discharge formula for $\widehat{q_b}$ must be in agreement with the physics of the problem: if $z_m = 0$, the solid transport discharge has to be 0. In this section we propose a new general formulation of the solid transport discharge that takes into account the thickness of the sediment moving layer. Let us consider a classical bedload solid transport discharge, written in the form (11). Then, using the notation of the previous section, we define the following solid transport discharge,

$$\widetilde{q_b}(h, hu, z_m) = z_m \alpha c\,(\tau_b^*)^{m_1}(\tau_b^* - \tau_{cr}^*)_+^{m_2-1}\mathrm{sgn}(\tau_b)\,Q, \tag{21}$$

where

$$\alpha = \frac{K_d}{K_e d_s}. \tag{22}$$

That is,

$$\widetilde{q_b}(h, hu, z_m) = z_m v_b \tag{23}$$

with

$$v_b = \alpha c\,(\tau_b^*)^{m_1}(\tau_b^* - \tau_{cr}^*)_+^{m_2-1}\,\mathrm{sgn}(\tau_b)\,Q. \tag{24}$$

3.1. Properties

Theorem 3.1. *The proposed formula (21) has the following properties:*

i) The formula depends explicitly on z_m and the continuity equation preserves the sediment mass.

ii) It coincides with a classical solid transport discharge in the case of a quasi-uniform regime.

Proof.

i) From (12), the conservation of sediment mass is obvious as whenever $z_m = 0$ we have that the solid flux is 0 which means that initial sediment mass is preserved in situations like the one described in Figure 3.

ii) In a quasi-uniform regime, the deposition rate equals the erosion rate ($\dot{z}_d = \dot{z}_e$), then from (17) and (20), we have that

$$\frac{z_m(1-\varphi)}{d_s} = \frac{K_e}{K_d}(\tau_b^* - \tau_{cr}^*)_+. \tag{25}$$

Note that $z_m(1-\varphi)/d_s$ represents a number of particles. Thus, whenever erosion and the deposition rates are equal, we may simplify the solid transport discharge (14),

$$\widehat{q_b} = z_m v_b = \frac{K_e d_s}{K_d}\frac{v_b}{(1-\varphi)}\,(\tau_b^* - \tau_{cr}^*)_+. \tag{26}$$

Replacing α and v_b by their respective values (22) and (24), we recover equation (11):

$$\widehat{q_b} = \frac{K_e d_s}{K_d}\frac{K_d}{K_e d_s}\frac{c}{(1-\varphi)}\,(\tau_b^*)^{m_1}(\tau_b^* - \tau_{cr}^*)_+^{m_2}\,\mathrm{sgn}(\tau_b)\,Q = q_b.$$

In this case we obtain a solid transport discharge that can be written without dependence on z_m.

□

Remark 3.1.
- *Charru et al. propose in [14] to define v_b in terms of $(\tau_b\, d_s/\mu)$ for viscous laminar flows. For turbulent flows v_b can be defined in terms of $\sqrt{\tau_b^*}$. Note that if we approximate v_b in terms of $\sqrt{(\tau_b^* - \tau_{cr}^*)_+}$ then we obtain that q_b is defined in terms of $(\tau^* - \tau_{cr}^*)^{3/2}$ corresponding, for example, to the Meyer-Peter & Müller or Fernández-Luque and Van Beek formulae.*

- *To obtain (26) we have used the relation (25). Actually, the relation between the number of particles of the moving layer and $(\tau_b^* - \tau_{cr}^*)_+$ is used in the deduction of some of the most known classical formulae for the solid transport discharge. Bagnold obtained such a linear relation by studying the momentum transfer due to the interaction of the particles with the fixed bed (see [25], [22]). At the fixed bed the fluid shear stress is reduced to the threshold value τ_{cr}. That is, the momentum transfer within the moving layer z_m is $(\tau_b^* - \tau_{cr}^*)_+$. That implies a limitation in the erosion rate. Consequently, a relation similar to (25) can be obtained. Moreover, such a linear relation has been also observed experimentally by Fernández-Luque and Van Beek (see [15]).*

Remark 3.2. *The solid transport discharge depends on the hydrodynamical variables only through the shear stress or the Shields parameter. Thus, in what follows, it will be useful to rewrite*

$$q_b \equiv \phi(\tau_b^*)\frac{sgn(\tau_b)}{1-\varphi}\,Q,$$

where

$$\phi(\tau_b^*) = c(\tau_b^*)^{m_1}(\tau_b^* - \tau_{cr}^*)^{m_2},$$

and

$$\widetilde{q_b} \equiv z_m v_b$$

with

$$v_b \equiv \alpha\frac{\phi(\tau_b^*)}{\tau_b^* - \tau_{cr}^*}sgn(\tau_b)Q.$$

To sum up, we have that the right hand side of the last two equations of (16) can be considered to be zero for uniform flows where the rate of erosion and deposition are equal. In this case we may consider a solid transport discharge formula that is independent of z_m (classical bedload transport flux). Consequently, if the rate of erosion and deposition are not equal, in the case of a non-uniform flow, definition of a solid transport discharge independent of z_m cannot be valid. For example, this is the case that we have shown in Figure 3, and that implies the non conservation of the sediment mass when classical formulae for $\widehat{q_b}$, independent of z_m, are applied.

3.2. Application to saturated flows

In this subsection we study the model defined by

$$\begin{cases} \partial_t h + \partial_x(hu) = 0, \\ \partial_t(hu) + \partial_x(hu^2 + gh^2/2) = -gh\partial_x(z_b + z_r), \\ \partial_t z_b + \partial_x \widehat{q_b} = 0, \\ (\mathrm{sgn}(\tau_b)\, l_s)\partial_x \widehat{q_b} + \widehat{q_b} = q_b. \end{cases} \tag{27}$$

where l_s is the saturation length. It is considered to introduce saturated effects in a classical model defined in terms of a solid transport discharge q_b. See for example [16], [17], [18], [26].
In what follows we see that model (27) can be obtained as a particular case of the one proposed in this paper, with a saturation length defined in terms of the erosion constant K_e.
Let us consider the erosion-deposition model that we propose, defined by (16) with $\widehat{q_b} = \widetilde{q_b}$ where $\widetilde{q_b}$ is given by (21). And assume that $\partial_x \widetilde{q_b} = \dot{z}_e - \dot{z}_d$, what implies $\partial_t z_m = 0$, that is, the flux is saturated. Then, by adding up the last two equations and by using this assumption we obtain the following system

$$\begin{cases} \partial_t z_b + \partial_x \widetilde{q_b} = 0, \\ \partial_x \widetilde{q_b} = \dot{z}_e - \dot{z}_d. \end{cases}$$

If we substitute the expressions (17), (20), and (23) the system becomes

$$\begin{cases} \partial_t z_b + \partial_x \widetilde{q_b} = 0, \\ \partial_x \widetilde{q_b} = \dfrac{-K_d V}{v_b d_s}\, \widetilde{q_b} + \dfrac{K_e V}{(1-\varphi)} (\tau_b^* - \tau_{cr}^*)_+. \end{cases} \tag{28}$$

If we denote

$$l_s = c\,(\tau_b^*)^{m_1} (\tau_b^* - \tau_{cr}^*)_+^{m_2 - 1} \frac{d_s}{K_e} \quad \text{and} \quad v_e = \frac{K_e V (\tau_b^* - \tau_{cr}^*)_+}{(1-\varphi)}, \tag{29}$$

then the second equation of system (28) can be expressed as

$$\partial_x \widetilde{q_b} = -\frac{\operatorname{sgn}(\tau_b)}{l_s} \widetilde{q_b} + v_e. \tag{30}$$

Finally, as we have the equality $l_s v_e = |q_b|$, we can rewrite (30) in the following form,

$$(\operatorname{sgn}(\tau_b)\, l_s) \partial_x \widetilde{q_b} + \widetilde{q_b} = q_b. \tag{31}$$

Equation (31) is an intrinsic property of the model we propose, namely system (15)-(21). Note that l_s can be seen as a relaxation parameter, which is inversely proportional to the erosion constant K_e. Several definitions of the saturation length l_s can be found in the literature, see for example [18], [16], [23]. It is estimated (see [27]) to be of the order of $(\rho_s/\rho) d_s$. It is obtained with definition (29) if, for example, K_e is proportional to (ρ/ρ_s).
And q_b can be seen as the equilibrium value towards which the solid transport discharge $\widetilde{q_b}$ converges. Let us remark that q_b is a classical bedload transport formula that here we write under the form of equation (11).

Remark 3.3. *If we are interested in a model of the form (27) to introduce saturated effects in a classical model defined by q_b, we can consider the following relaxation version of the model,*

$$\begin{cases} \partial_t h + \partial_x (hu) = 0, \\ \partial_t (hu) + \partial_x (hu^2 + gh^2/2) = -gh \partial_x (z_m + z_f + z_r), \\ \partial_t z_m = \dfrac{1}{\varepsilon} \Big(- \partial_x \widetilde{q_b} + \dot{z}_e - \dot{z}_d \Big), \\ \partial_t z_f = -\dot{z}_e + \dot{z}_d. \end{cases}$$

being ε the relaxation parameter and $\widetilde{q_b}$ defined by (21) in terms of the given classical solid transport discharge formula q_b.

4. Eigenvalues of Exner system for modified bedload transport formulae

We are interested in the study of the eigenvalues of system (16). The PDE system (16) can be written in vectorial form as

$$\partial_t \widetilde{W} + \partial_x \widetilde{F}(W) = \widetilde{B}(W) \partial_x \widetilde{W} + \widetilde{S}(W) \partial_x z_r + \widetilde{G}, \tag{32}$$

where

$$W = \begin{pmatrix} h \\ q \\ z_m \end{pmatrix} \in \mathbb{R}^3, \quad \widetilde{W} = \begin{pmatrix} W \\ \hline z_f \end{pmatrix} \in \mathbb{R}^4$$

is the state vector in conservative form, where $q = hu$, and

$$\tilde{F}(W) = \begin{pmatrix} F(W) \\ \hline 0 \end{pmatrix}, \quad F(W) = \begin{pmatrix} hu \\ hu^2 + \dfrac{g}{2} h^2 \\ z_m v_b(h, hu) \end{pmatrix}, \quad \widetilde{B}(W) = \left(\begin{array}{c|c} B(W) & S(W) \\ \hline 0 & 0 \end{array} \right),$$

$$B(W) = \begin{pmatrix} 0 & 0 & 0 \\ 0 & 0 & -gh \\ 0 & 0 & 0 \end{pmatrix}, \quad S(W) = \begin{pmatrix} 0 \\ -gh \\ 0 \end{pmatrix}, \quad \widetilde{S}(W) = \begin{pmatrix} S(W) \\ \hline 0 \end{pmatrix},$$

$$\widetilde{G} = \begin{pmatrix} G \\ \hline -\dot{z}_e + \dot{z}_d \end{pmatrix}, \quad G = \begin{pmatrix} 0 \\ 0 \\ \dot{z}_e - \dot{z}_d \end{pmatrix}.$$

The definition of $v_b(h, q)$ can be considered following the proposed model by (24). Let us remark that with these notations system (32) can be rewritten as

$$\begin{cases} \partial_t W + \partial_x F(W) = B(W)\partial_x W + S(W)\partial_x(z_r + z_f) + G, \\ \partial_t z_f = -\dot{z}_e + \dot{z}_d. \end{cases} \tag{33}$$

System (32) can also be written in quasi-linear form as

$$\partial_t \widetilde{W} + \widetilde{A}(W)\partial_x \widetilde{W} = \widetilde{S}(W)\partial_x z_r + \widetilde{G}$$

where $\widetilde{A}(W) = D_{\widetilde{W}}\widetilde{F} - \widetilde{B}(W)$ is the matrix of transport coefficients. More explicitly, taking into account that $v_b = v_b(\tau_b)$ with $\tau_b \equiv \tau_b(h, q)$, we have

$$\widetilde{A}(W) = \left(\begin{array}{c|c} A(W) & S(W) \\ \hline 0 & 0 \end{array}\right)$$

where $A(W) = D_W F(W) - B(W)$,

$$A(W) = \begin{pmatrix} 0 & 1 & 0 \\ gh - u^2 & 2u & gh \\ z_m \dfrac{\partial v_b}{\partial h} & z_m \dfrac{\partial v_b}{\partial q} & v_b \end{pmatrix}. \tag{34}$$

An important property of such systems is hyperbolicity [28] which requires that the matrix $\widetilde{A}(W)$ is $\mathbf{R}$ diagonalizable (or strictly hyperbolic when eigenvalues are distinct). Given the definition of $\widetilde{A}(W)$, we are concerned whether $A(W)$ is diagonalizable.
In what follows, we shall consider a classical bedload transport flux q_b in the form (11) and we shall assume that q_b satisfies the following hypothesis:

- The solid transport flux is an increasing function of the discharge

$$\frac{\partial q_b}{\partial q} \geq 0, \tag{H1}$$

- There exists a constant $k > 0$ such that

$$\frac{\partial q_b}{\partial h} = -k\frac{q}{h}\frac{\partial q_b}{\partial q}. \tag{H2}$$

Remark 4.1.

- *(H1) is equivalent to* $\dfrac{\partial \tau_b}{\partial q} \geq 0$

  To show this, remark that from (3) we have

  $$\tau_b^* = \beta|\tau_b|,$$

  where $\beta = ((\rho_s - \rho)gd_s)^{-1}$ *and*

  $$\partial\tau_b^* = \beta sgn(\tau_b)\partial\tau_b.$$

  Now, considering the case $\tau_b^* > \tau_{cr}^*$*, (the other case being trivial), we have*

  $$\frac{\partial q_b}{\partial q} = k\left(m_1(\tau_b^* - \tau_{cr}^*) + m_2\tau_b^*\right)(\tau_b^*)^{m_1-1}(\tau_b^* - \tau_{cr})^{m_2-1}\beta\frac{\partial \tau_b}{\partial q}, \tag{35}$$

  and the result follows.

- *(H2) is equivalent to*

$$\frac{\partial \tau_b}{\partial h} = -k\frac{q}{h}\frac{\partial \tau_b}{\partial q}.$$

This can be easily shown by comparing (35) with

$$\frac{\partial q_b}{\partial h} = k\left(m_1(\tau_b^* - \tau_{cr}^*) + m_2\tau^*\right)(\tau_b^*)^{m_1-1}(\tau_b^* - \tau_{cr})^{m_2-1}\beta\frac{\partial \tau_b}{\partial h}.$$

- *In [29], it was shown that classical formulae satisfy in general the relation*

$$\frac{\partial q_b}{\partial h} = -k\frac{q}{h}\frac{\partial q_b}{\partial q}, \tag{36}$$

where k is a given positive constant. For instance, for Grass model [9] we have $k = 1$ and for Meyer-Peter&Müller [10] we have $k = 7/6$.

Proposition 4.1. *Consider any classical flux q_b in the form (11) that satisfies (H1) and (H2), then v_b given by (24) satisfies*

- $\dfrac{\partial v_b}{\partial q} \geq 0$
- $\dfrac{\partial v_b}{\partial h} = -k\dfrac{q}{h}\dfrac{\partial v_b}{\partial q}$

Proof. From Remark 3.2, a simple calculation shows

$$\partial v_b = \alpha\frac{\phi'(\tau_b^*)(\tau_b^* - \tau_{cr}^*) - \phi(\tau_b^*)}{(\tau_b^* - \tau_{cr}^*)^2}\beta\partial\tau_b^*$$

and from (H1) - (H2) the result follows.

□

As a consequence, the matrix $A(W)$ defined by (34) can be written as

$$A(W) = \begin{pmatrix} 0 & 1 & 0 \\ gh - u^2 & 2u & gh \\ -kub & b & v_b \end{pmatrix}, \tag{37}$$

where $b = z_m\dfrac{\partial v_b}{\partial q}$.
The characteristic polynomial of $A(W)$ can then be written as

$$\begin{aligned} p_A(\lambda) = &\quad (v_b - \lambda)\begin{vmatrix} -\lambda & 1 \\ -u^2 + gh & 2u - \lambda \end{vmatrix} - gh\begin{vmatrix} -\lambda & 1 \\ -kub & b \end{vmatrix} \\ = &\quad (v_b - \lambda)[(u-\lambda)^2 - gh)] + ghb(\lambda - ku). \end{aligned} \tag{38}$$

In what follows, let us denote by

$$\{\mu_1, \mu_2, \mu_3\} = \{v_b, u \pm \sqrt{gh}\} \qquad \text{with} \qquad \mu_1 < \mu_2 < \mu_3.$$

System (32) is thus strictly hyperbolic if and only if $p_A(\lambda)$ has three different solutions noted by $\lambda_1 < \lambda_2 < \lambda_3$. In other words if the curve $f(\lambda) = (\lambda - v_b)[(u-\lambda)^2 - gh)]$ and the line $d(\lambda) = ghb(\lambda - ku)$ have three distinct points of intersection (see Figure 4). We have the following result:

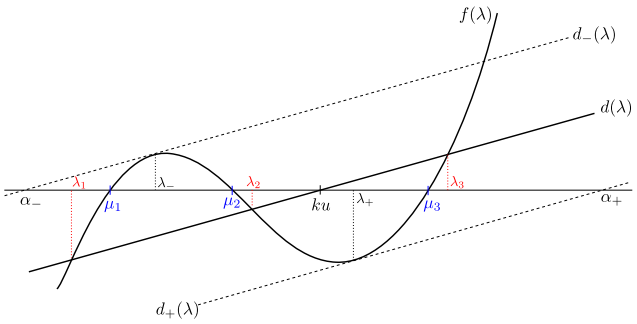

Figure 4: Hyperbolicity of Exner system

Proposition 4.2. *Consider system (32) with (11) satisfying (H1) - (H2). For a given state (h, q), the system is strictly hyperbolic if and only if*

$$\alpha_- < ku < \alpha_+,$$

where $\alpha_\pm$ will be defined later by expression (41). More explicitly,

- *In the case $k = 1$, the system is always strictly hyperbolic.*
- *In the case $k = 7/6$, a sufficient condition for system (32) to be strictly hyperbolic is*

$$|u| < 6\sqrt{gh}.$$

□

Let us remark that we obtain a similar result to the case where bedload sediment transport formula does not depend on z_m, as it is shown in [29]. The proof is not exactly the same but can be done by following similar steps as in [29]. The proof is included in Appendix A for the sake of completeness.

We are interested in classifying the different roots of the polynomial $p_A(\lambda)$. More explicitly, in the case of classical bedload transport flux, it is a known fact (see [29] and references therein) that we have always two eigenvalues of the same sign and a third one of opposite sign. We intend to show that the behaviour with the modified bedload flux (21) is quite different. Assume that the system is strictly hyperbolic and denote by $\lambda_1 < \lambda_2 < \lambda_3$ the three roots of $p_A(\lambda)$.
Remark that (38) may be written in the form

$$p_A(\lambda) = -\lambda^3 + a_2\lambda^2 + a_1\lambda + a_0,$$

where a_0, a_1, a_2 are the corresponding coefficients of the polynomial. In what interests us, we remark that

$$a_0 = v_b(u^2 - gh) - kbhug.$$

Moreover, we also have $p_A(\lambda) = -(\lambda - \lambda_1)(\lambda - \lambda_2)(\lambda - \lambda_3)$ and $a_0 = \lambda_1\lambda_2\lambda_3$.
We have 4 different cases:

Case 1: $0 < \mu_1$. Then two possibilities arise (see Figure 5)

- $a_0 < 0$. We have two positive eigenvalues and one negative (Figure 5(a))
- $a_0 > 0$. We have three positive eigenvalues (Figure 5(b)))

Remark that $a_0 > 0$ is equivalent to

$$1 < \frac{v_b(u^2 - gh)}{kbhug} = \frac{v_b(u^2 - gh)}{kz_m\dfrac{\partial v_b}{\partial(hu)}hug}.$$

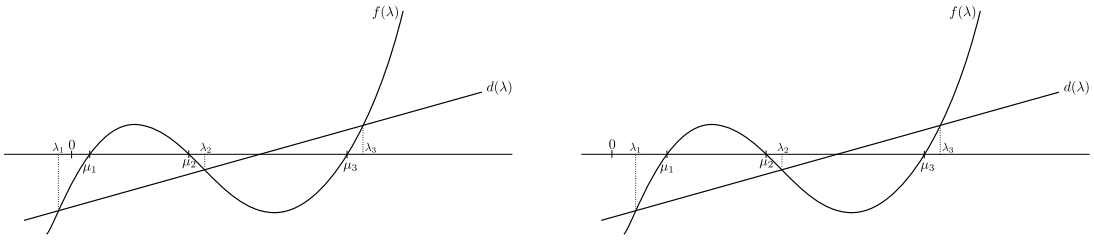

(a) (b)

Figure 5: Case $0 < \mu_1$

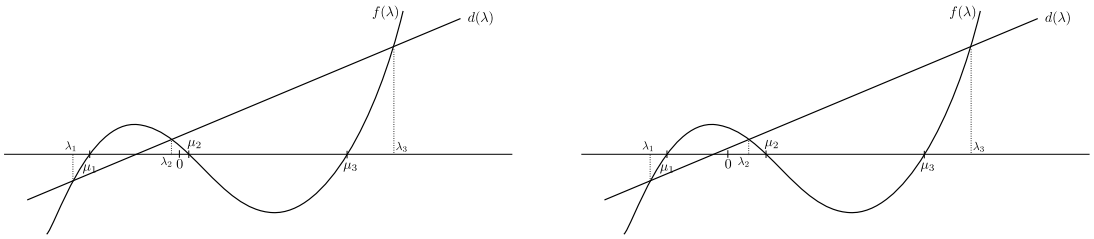

(a) (b)

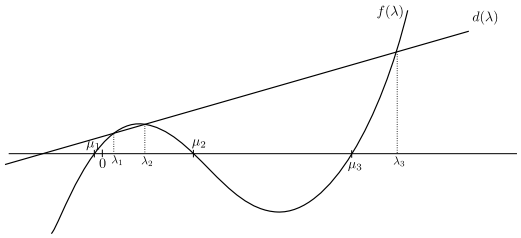

(c)

Figure 6: Case $\mu_1 < 0 < \mu_2 < \mu_3$

As $\mu_1 > 0$, we are in a supercritical regime $u^2 - gh > 0$. Moreover, $v_b/(hu) > 0$ and $\dfrac{\partial v_b}{\partial (hu)} > 0$. Thus

$$z_m < \frac{v_b(u^2 - gh)}{k \dfrac{\partial v_b}{\partial (hu)} hug}$$

is satisfied if and only if z_m is small enough.

Case 2: $\mu_1 < 0 < \mu_2 < \mu_3$. Then we have three possibilities:

- $\lambda_1 < \lambda_2 < 0 < \lambda_3$ (Figure 6(a))
- $\lambda_1 < 0 < \lambda_2 < \lambda_3$ (Figure 6(b))
- $0 < \lambda_1 < \lambda_2 < \lambda_3$ (Figure 6(c))

But now remark that $\mathrm{sgn}(v_b) = \mathrm{sgn}(u)$, and as $\mu_1 < 0 < \mu_2 < \mu_3$, we have necessarily $u > 0$ (otherwise we would have $v_b < 0$ and $u - \sqrt{gh} < 0$). This means that we are in a subcritical regime $u^2 - gh < 0$,

$$a_0 = v_b(u^2 - gh) - kbhug < 0,$$

and $\mathrm{sgn}(a_0) = \mathrm{sgn}(\lambda_1 \lambda_2)$. As a consequence, the only possible case is $\lambda_1 < 0$ and $\lambda_2, \lambda_3 > 0$.

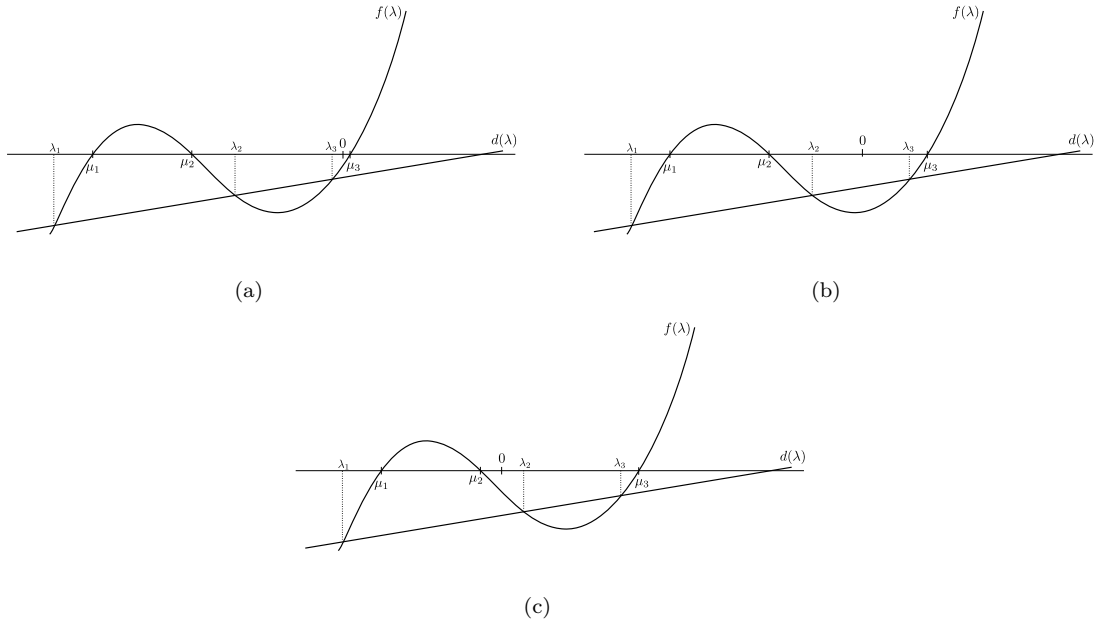

(a) (b)

(c)

Figure 7: Case $\mu_1 < \mu_2 < 0 < \mu_3$

Case 3: $\mu_1 < \mu_2 < 0 < \mu_3$ Then we have three possibilities (Figure 7)

- $\lambda_1 < \lambda_2 < \lambda_3 < 0$ (Figure 7(a))
- $\lambda_1 < \lambda_2 < 0 < \lambda_3$ (Figure 7(b))
- $\lambda_1 < 0 < \lambda_2 < \lambda_3$ (Figure 7(c))

As $\text{sgn}(v_b) = \text{sgn}(u)$ we should have $u < 0$, otherwise we would have $u + \sqrt{gh} > 0$ and $v_b > 0$. This means we are in a subcritical region $u^2 - gh < 0$. Thus

$$a_0 = v_b(u^2 - gh) - kbhug > 0,$$

and we have $\text{sgn}(a_0) = -\text{sgn}(\lambda_2\lambda_3)$. As a consequence the only possible case is $\lambda_1, \lambda_2 < 0$ and $\lambda_3 > 0$.

Case 4: $\mu_1 < \mu_2 < \mu_3 < 0$ Then two possibilities arise (see Figure 8)

- $a_0 < 0$. We have two negative eigenvalues and one positive (Figure 5(a))
- $a_0 > 0$. We have three negative eigenvalues (Figure 5(b)))

Remark that $a_0 > 0$ is equivalent to

$$1 < \frac{v_b(u^2 - gh)}{kbhug} = \frac{v_b(u^2 - gh)}{kz_m \dfrac{\partial v_b}{\partial(hu)} hug}.$$

In this case, we have $u^2 - gh > 0$ (supercritical regime) and $a_0 > 0$ is equivalent to

$$\frac{v_b(u^2 - gh)}{k \dfrac{\partial v_b}{\partial(hu)} hug} > z_m,$$

which is satisfied if and only if z_m is small enough.

To summarize the results:

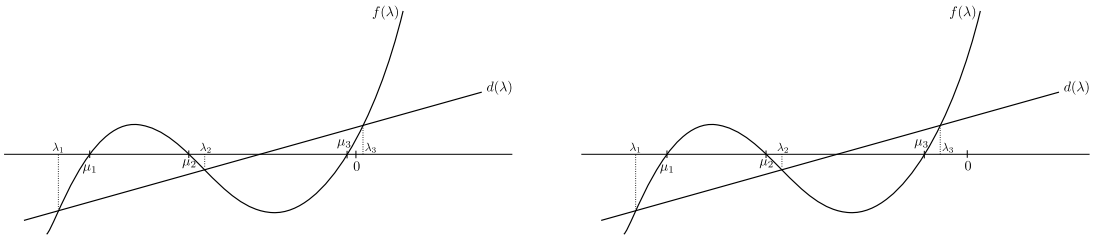

(a) (b)

Figure 8: Case $\mu_1 < \mu_2 < \mu_3 < 0$

- In the subcritical case ($u^2 - gh < 0$), we have two eigenvalues of the same sign and one of opposite sign.
- In the supercritical case ($u^2 - gh > 0$), we have two possibilities:
  - Three eigenvalues of the same sign,
  - Two eigenvalues of the same sign and one of opposite sign.

Remark that the supercritical region presents a major difference compared to classical bedload transport formulae. In the classical case, we always have two eigenvalues of the same sign and one of different sign, but here there is a new possibility of having three eigenvalues of the same sign due to the new solid transport discharge.
In Section 2 we have presented two forms to obtain a solid transport discharge depending on z_m. The first one, was proposed by Fowler et al. in [19] as an extension of the Meyer-Peter & Müller formula. Although the idea can be easily extended for other classical models. The second one has been proposed at the end of Section 2. If we consider a classical model that can be written as

$$q_b(h,u) = c\,(\tau_b^*)^{m_1}(\tau_b^* - \tau_{cr}^*)_+^{m_2},$$

then, we can resume both models as follows,

$$\widetilde{q}(h,u,z_b) = z_m v_b,$$

with v_b defined as follows:

- In the case of the extension proposed by Fowler et al. we have:

$$v_b = c_1(\tau_b^*)^{m_1}(\tau_b^* - \tau_{cr}^*)_+^{m_2}.$$

- In the case of the extension proposed in Section 2 we have:

$$v_b = c_2\,(\tau_b^*)^{m_1}(\tau_b^* - \tau_{cr}^*)_+^{m_2-1},$$

being c_1 and c_2 two different constant values. The value of these constants does not have any influence on the condition

$$z_m < \frac{v_b(u^2-gh)}{k\dfrac{\partial v_b}{\partial(hu)}hug}. \tag{39}$$

In order to study the influence of the considered model in condition (39), it is enough to study the ratio $v_b/\frac{\partial v_b}{\partial(hu)}$. When we consider the extension proposed by Fowler et al. we obtain,

$$\frac{v_b}{\frac{\partial v_b}{\partial(hu)}} = \frac{1}{2}\frac{hu}{m_1 + m_2\frac{\tau_b^*}{(\tau_b^*-\tau_{cr}^*)_+}}.$$

For the model proposed in Section 2 we obtain the same result but by substituting m_2 by $m_2 - 1$. Consequently, if we consider the Meyer-Peter & Müller formula, corresponding to $m_1 = 0$, $m_2 = 3/2$, we obtain that the maximum value of z_m verifying condition (39) for the case of the model proposed by Fowler et al. is 3 times smaller than for the case of the model proposed in Section 2.

5. Numerical results

5.1. Numerical approach by finite volume methods

As usual, we consider a set of computing cells $I_i = [x_{i-1/2}, x_{i+1/2}], i \in \mathbb{Z}$. We shall assume that these cells have a constant size $\triangle x$ and that $x_{i+1/2} = i\triangle x$. The point $x_i = (i-1/2)\triangle x$ is the center of the cell I_i. Let $\triangle t$ be the time step and $t^n = n\triangle t$.

We denote by $W_i^n = (h_i^n, q_i^n, z_{m,i}^n)^T$ the approximation of the cell averages of the exact solution

$$W_i^n \cong \frac{1}{\triangle x}\int_{x_{i-1/2}}^{x_{i+1/2}} W(x,t^n)dx,$$

and

$$H_i^n = z_{f,i}^n + z_{r,i}, \quad \text{with} \quad z_{f,i}^n \cong \frac{1}{\triangle x}\int_{x_{i-1/2}}^{x_{i+1/2}} z_f(x,t^n)dx, \quad z_{r,i} \cong \frac{1}{\triangle x}\int_{x_{i-1/2}}^{x_{i+1/2}} z_r(x)dx.$$

We propose a two-step numerical scheme to treat the transference terms between the static layer and the rolling particles layer.

Let us suppose that the values W_i^n and H_i^n are known. In order to advance in time we proceed as follows:

- **First Step.** We define $W_i^{n+1/2} = (h_i^{n+1/2}, q_i^{n+1/2}, z_{m,i}^{n+1/2})^T$ as

$$W_i^{n+1/2} = W_i^n - \frac{\Delta t}{\Delta x}\big(D_{i-1/2}^{n,+} + D_{i+1/2}^{n,-}\big),$$

where $D_{i+1/2}^{n,\pm} = D(W_i^n, W_{i+1}^n, H_i^n, H_{i+1}^n)^{\pm}$, being

$$D(W_i, W_{i+1}, H_i, H_{i+1})^{\pm} = \frac{1}{2}\left(I \pm \operatorname{sgn}(A_{i+1/2})\right)\left(F(W_{i+1}) - F(W_i) + B_{i+1/2}(W_{i+1} - W_i) + S_{i+1/2}(H_{i+1} - H_i)\right).$$

where I is the identity matrix and $\operatorname{sgn}(A_{i+1/2})$ is the matrix sign of $A_{i+1/2}$. Moreover,

$$B_{i+1/2} = B\left(\frac{W_i + W_{i+1}}{2}\right), \quad S_{i+1/2} = S\left(\frac{W_i + W_{i+1}}{2}\right)$$

and

$$A_{i+1/2} = \begin{pmatrix} 0 & 1 & 0 \\ gh_{i+1/2} - u_{i+1/2}^2 & 2u_{i+1/2} & gh_{i+1/2} \\ -ku_{i+1/2}b_{i+1/2} & b_{i+1/2} & v_{b,i+1/2} \end{pmatrix},$$

is assumed to be a Roe matrix for (33) in the particular case that

$$\frac{\partial q_b}{\partial h} = -k\frac{q}{h}\frac{\partial q_b}{\partial q},$$

that is a Roe matrix in the form (37). In particular, the usual definitions

$$h_{i+1/2} = \frac{h_i + h_{i+1/2}}{2}, \quad u_{i+1/2} = \frac{\sqrt{h_i}u_i + \sqrt{h_{i+1}}u_{i+1}}{\sqrt{h_i} + \sqrt{h_{i+1}}},$$

are taken, which corresponds to the choice of segments as the path connecting two different states. See [30, 31, 32] for further details. As it was stated in [5] it is possible to write a Roe matrix for the Grass model. Nevertheless, it is not possible or it is very costly to write a Roe matrix for other models, such as Meyer-Peter&Müller or some other models considered in this work. So, in practice the following approximation is used

$$b_{i+1/2} = \frac{z_{m,i} + z_{m,i+1}}{2}\frac{\partial q_b}{\partial(hu)}(h_{i+1/2}, h_{i+1/2}u_{i+1/2}).$$

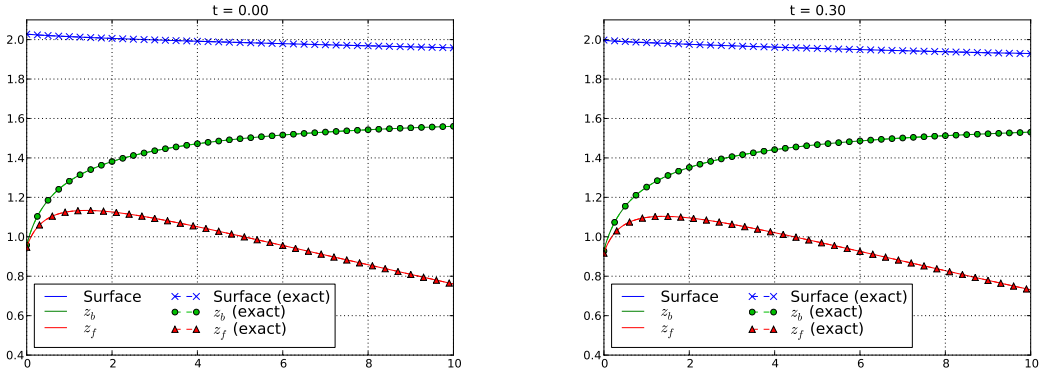

(a) Initial conditions

(b) Solution at $t = 0.3$

Figure 9: Comparison between the approximate and the analytic solution: free surface, bottom surface (z_b) and layer of sediments that are not moving (z_f)

- **Second step.**

  We define

$$W_i^{n+1} = (h_i^{n+1/2}, q_i^{n+1/2}, z_{m,i}^{n+1})^T, \quad H_i^{n+1} = z_{f,i}^{n+1} + z_{r,i},$$

  where

$$\begin{cases} z_{m,i}^{n+1} &= z_{m,i}^n + \Delta t(\dot{z}_{e,i}^{n+1/2} - \dot{z}_{d,i}^{n+1/2}), \\ z_{f,i}^{n+1} &= z_{f,i}^n + \Delta t(-\dot{z}_{e,i}^{n+1/2} + \dot{z}_{d,i}^{n+1/2}), \end{cases}$$

  and $\dot{z}_{e,i}^{n+1/2} = \dot{z}_{e,i}(W_i^{n+1/2})$, $\dot{z}_{d,i}^{n+1/2} = \dot{z}_{d,i}(W_i^{n+1/2})$.

5.2. Numerical tests

All the numerical tests have been performed with 800 finite volumes.

5.2.1. Validation thanks to an analytical solution

In the spirit of [33], we obtained a family of analytical solutions, given by equations (43)–(44). The derivation is detailed in Appendix B. With these solutions, we validate our code for the new bedload formula. We plot in Figure 9 the analytical solution and the approximate solution for $q = 0.5$, $A = 0.1$, $B = 0.005$, $C = 0.1$, $K_d = 1$, $K_e = 1$, $V = 5 \cdot 10^{-3}$ m/s, $d_s = 5.8 \cdot 10^{-3}$ m, $\varphi = 0$, $m_2 = 3/2$, $C_1 = 100$ and $\left(\frac{u^2}{2} + g\,(h + z_b)\right)_{|t=0} = 20$ (recall that $m_1 = 0$, $z_r = 0$ and $\tau_{cr}^* = 0$). On the left boundary, we impose $q = 0.5$ and $z_m = 0.0107$, and on the right boundary the discharge is fixed $q = 0.5$.
The two solutions (exact and approximate) coincide.

5.2.2. Erosion and deposition rates for a dune

The goal of this test is to study the respective localizations of erosion and deposition. In [26], the authors claims that bumps and upwind slopes get more eroded than dips and downwind faces; that is what we want to check.
We choose to run the code over a submerged dune over a flat bottom. More precisely, we take the following parameters: we consider (6) and a Manning formula with coefficient $n = 0.04$, the characteristic velocity $V = 10^{-3}$ m/s; the porosity is $\varphi = 0$, the densities are $\rho = 1000$ kg/m^3 for the water and $\rho_s = 2612.9$ kg/m^3 for the sediments, and the diameter of the sediments is $d_s = 5.8 \cdot 10^{-5}$ m. For the bedload transport formula (11), we take $c = 8$, $m_1 = 0$ and $m_2 = 3/2$, and, for the erosion and deposition rates, we take $K_d = 0.1$ and $K_e = 1$.

We start from a stationary state for Shallow Water, namely the subcritical solution of:

$$\begin{cases} q = 0.5, \\ \dfrac{u^2}{2} + g\,(h + z_b) = 10.42, \end{cases}$$

and we impose the value of $q = 0.5$ on the left boundary.
The bottom z_b is chosen as $z_{b|t=0} = 0.1 + 0.1 \exp\left(-(x-5)^2\right)$, without non-erodible fixed layer ($z_r = 0$), and we take $z_{m|t=0} = \frac{K_e}{K_d} d_s \left(\tau^*_{b\,|t=0} - \tau^*_{cr}\right)_+$ in order to even out erosion and deposition at the initial time.

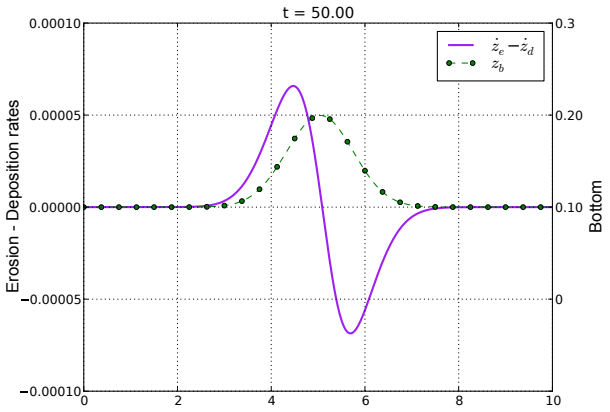

Figure 10: Erosion and deposition rates for a dune (left axis). Bottom is drawn (right axis) to show its influence

We give in Figure 10 the results at time $t = 50$ s. The difference between erosion and deposition rates is drawn. A positive value means that erosion is predominant, whereas when the value is negative, deposition is predominant. The dashed line represents the values of the bottom z_b (values given by the right scale). As said by Andreotti et al., erosion is predominant on the left part of the dune, and deposition is effective on the right part of the dune.

5.2.3. Comparison with the classical formula for a dune
We complete the previous numerical case with a comparison with the classical formula for the solid transport discharge (the parameters remain unchanged). We present in Figure 11 the results at times 300 s, 1000 s, 2000 s, 4000 s with the two formulations for the solid discharge.
We notice that the new formulation is more realistic than the classical one. On the right part of the dune indeed, the straight line given by the classical model is not physical, which is corrected by the deposition in the proposed model.
We can also plot the boundary between the layer of moving particles and the layer of sediments that are not moving, see Figure 12.

5.2.4. Case of a rectangular dune: value of τ^*_{cr}
We carry on the numerical tests with a rectangular dune, as in [5]. When we consider a value τ^*_{cr}, we observe that there is a point at the beginning of the dune that distinguish into two different zones: the part of the dune that does not move and the one that is moving. The goal of this test is to study this point, which we may call the rupture point, and its relation with the value of τ^*_{cr}.
For this numerical experiment, we consider Darcy-Weisbach friction term with $f = 0.1$, the characteristic velocity $V = 10^{-2}$ m/s; the porosity is $\varphi = 0$, and the diameter of the sediments is $d_s = 5.8{\cdot}10^{-2}$ m. For the bedload transport formula (11), we take $c = 8$, $m_1 = 0$ and $m_2 = 3/2$, and, for the erosion and deposition rates, we take $K_d = 0.1$ and $K_e = 1$.

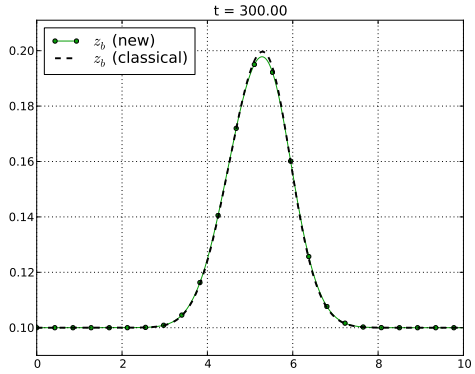

(a) Comparison at $t = 300$ s

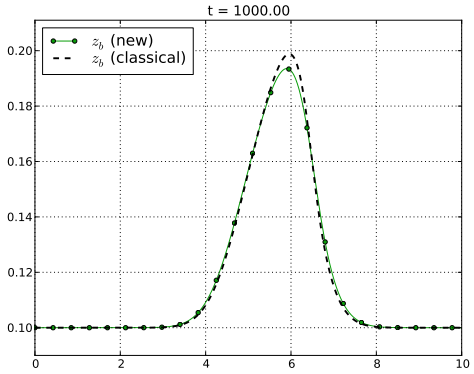

(b) Comparison at $t = 1000$ s

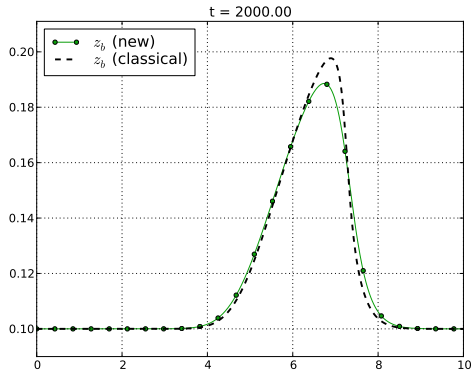

(c) Comparison at $t = 2000$ s

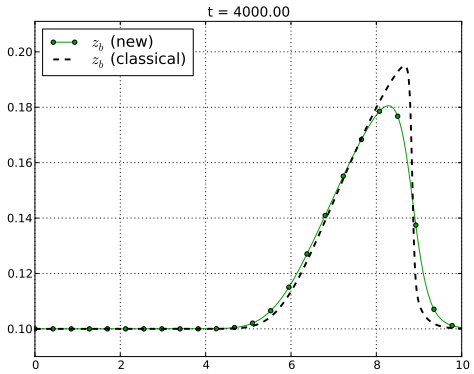

(d) Comparison at $t = 4000$ s

Figure 11: Bottom surface (z_b) with the new and classical bed load transport formulae for the evolution of a dune

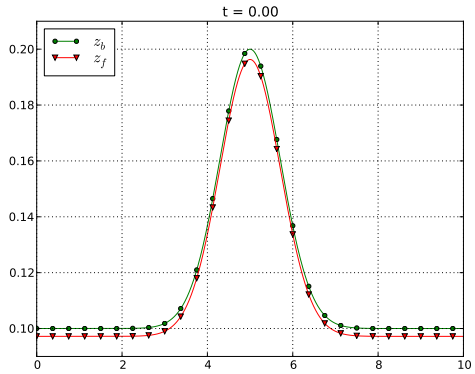

(a) Bottom at $t = 0$ s

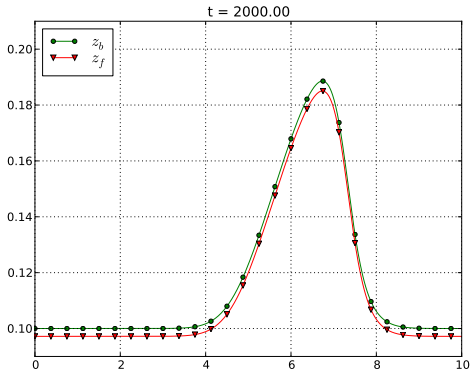

(b) Bottom at $t = 2000$ s

Figure 12: Bottom surface (z_b) and layer of sediments that are not moving (z_f) with the new bed load transport formula for the evolution of a dune

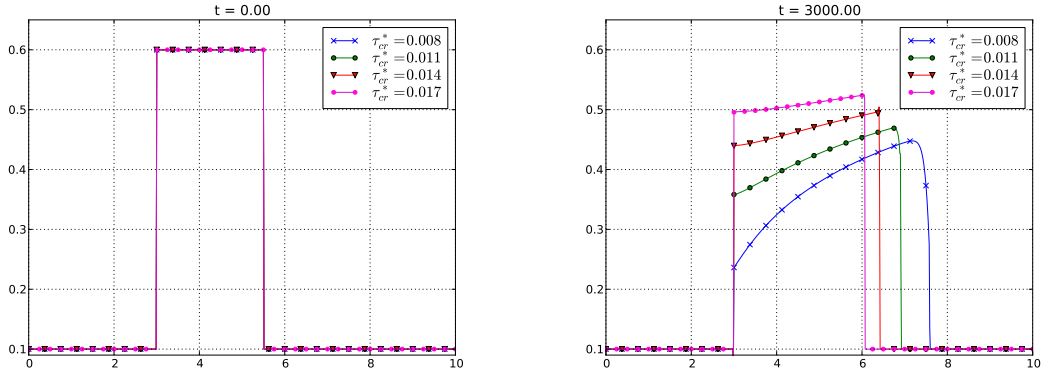

(a) Bottom at $t = 0$ s

(b) Bottom at $t = 3000$ s

Figure 13: Bottom surface (z_b) with the new bed load transport formula for the evolution of a rectangular dune, with three different values of τ_{cr}^*

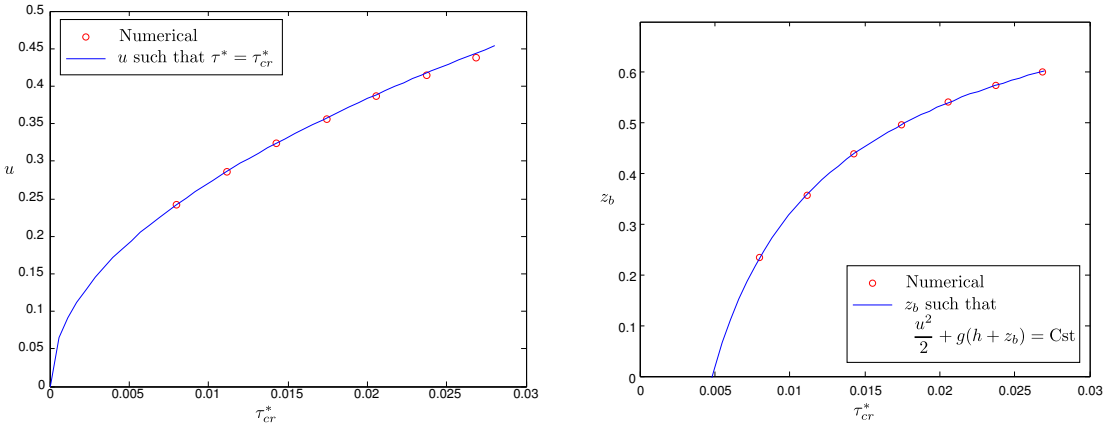

(a) u at $x = 3$

(b) z_b at $x = 3$

Figure 14: Comparison between theoretical an numerical values at rupture point $x = 3$

The initial conditions are given by the subcritical solution of

$$\begin{cases} q = 0.2, \\ \dfrac{u^2}{2} + g\,(h + z_b) = 10.42, \end{cases} \tag{40}$$

with $z_m = 0$, $z_r = 0$ and $z_b = 0.1 + 0.5 \cdot \mathbb{1}_{[4,6]}(x)$. We impose $q = 0.2$ on the left boundary, and we run several tests with τ_{cr}^* varying from 0.008 to 0.027, see Figure 13.
At the rupture point, which is located at $x = 3$, one expects that $\tau_b^* = \tau_{cr}^*$ for long times and that the shallow water relations (40) are satisfied. This is shown in Figure 14. Remark that these relations are equivalent for the classical and new model.

We have also performed this test for a non-trivial z_r, given by $z_r = 0.5 - 0.01x$, with $z_f = 0.15 \cdot \mathbb{1}_{[3,5]}(x)$, $z_m = 0.05 \cdot \mathbb{1}_{[3,5]}(x)$. The values of the parameters are: $d_s = 5.8 \cdot 10^{-4}$ m, $V = 10^{-3}$ m/s, $K_d = 0.5$ and $K_e = 5$, $c = 40$, $m_1 = 0$, $m_2 = 3/2$ and $\tau_{cr}^* = 0.5$. On the left boundary, we impose $q = 0.25$ and $z_m = 0$, and the initial solution satisfies

$$\begin{cases} q = 0.25, \\ \dfrac{u^2}{2} + g\,(h + z_b) = 10. \end{cases}$$

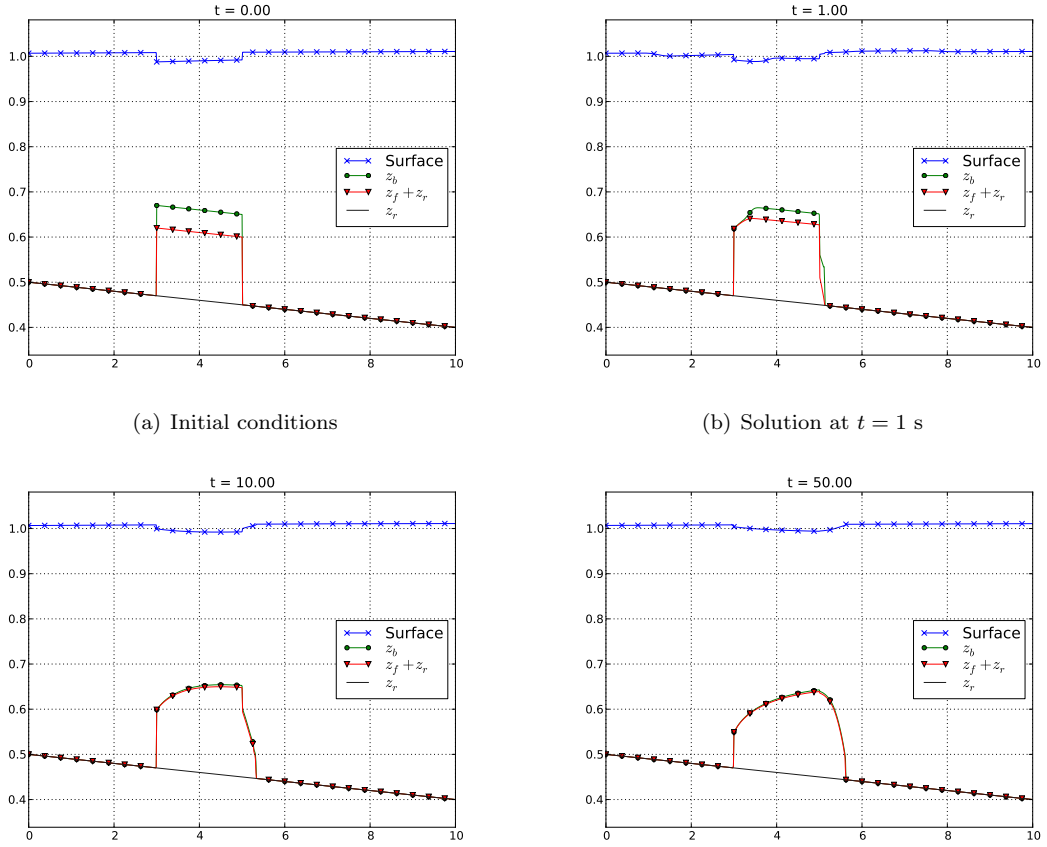

(a) Initial conditions

(b) Solution at $t = 1$ s

(c) Solution at $t = 10$ s

(d) Solution at $t = 50$ s

Figure 15: Free surface, bottom surface (z_b), layer of sediments that are not moving (z_f) and bedrock layer (z_r) with the new bed load transport formula for the evolution of a rectangular dune on an inclined plane

The results are given in Figure 15, and we can see erosion effects on the left part of the dune, deposition effects on the right part. More precisely, this test shows several results. First, starting from a quite large moving layer ($z_m = 0.05$ m while the dune is 0.2 m high), the moving layer becomes smaller to attain a size of the order of the diameter of grains. Concerning the profile of the dune, the front was sharp at the initial time but, thanks to deposition, the layer of sediments that are not moving (z_f) increases and it creates a smooth profile. This test also illustrates the obtention of the rupture point at $x = 3$.

5.2.5. Eigenvalues in a supercritical case

In this section, we give examples to illustrate the sign of eigenvalues for supercritical flows. We proved in section 4 that in the classical case, we always have two eigenvalues of the same sign and one of different sign, but here there is a new possibility of having three eigenvalues of the same sign due to the new solid transport discharge.

The first results are given in Figures 16–17: we plot the eigenvalues for a supercritical case where both transport discharges have the same behavior, namely two eigenvalues of the same sign and one of different sign. The parameters are the following: $\rho = 1000$ kg/m^3, $\rho_s = 2612.9$ kg/m^3, $d_s = 5.8 \cdot 10^{-3}$ m, $n = 0.04$, $\tau_{cr} = 0$, $V = 10^{-3}$ m/s, $c = 8$, $K_d = 0.1$, $K_e = 1$. The topography is taken as $z_b = 0.5 + 0.1\exp(-(x-5)^2)$, $z_m = 0.45$, and $z_f = z_b - z_m$ ($z_r = 0$), $\varphi = 0$, $m_1 = 0$,

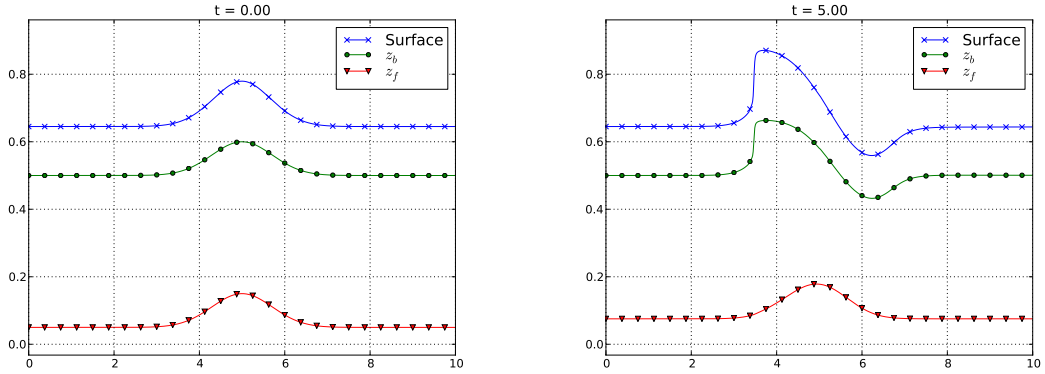

(a) Initial conditions

(b) Solution at $t = 5$

Figure 16: Free surface, bottom surface (z_b) and layer of sediments that are not moving (z_f) in a supercritical case for which there are two positive and one negative eigenvalues with the new bed load transport discharge

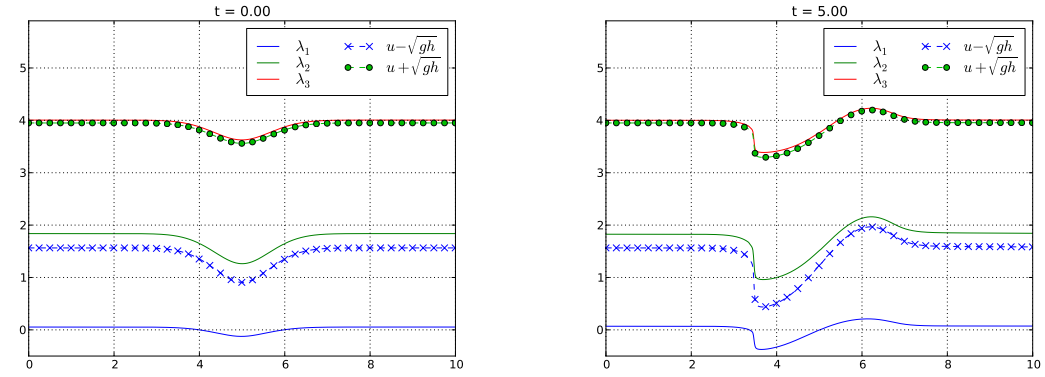

(a) Eigenvalues $t = 0$

(b) Solution at $t = 5$

Figure 17: Comparison between the eigenvalues of System (16) and the one of the Shallow-Water system in a supercritical case for which there are two positive and one negative eigenvalues with the new bed load transport discharge

$m_2 = 3/2$ and the flow is initially defined by

$$\begin{cases} q = 0.4, \\ \dfrac{u^2}{2} + g\,(h + z_b) = 10.13. \end{cases}$$

Open boundary conditions have been used.
We also run another test where we only change the value of z_m: $z_m = 0.1$. In this case, we obtain three positive eigenvalues, see Figures 18–19. This configuration cannot be obtained with a classical formula for the transport discharge.

6. Conclusions

We have introduced a general formulation for solid transport flux that takes into account the thickness of the sediment layer. Compared to classical formulae this one has the advantage of preserving sediment mass in situations where sediment is isolated inside the considered domain. This new formulation reduces to the classical one when we consider quasi-uniform regimes. Moreover, it considers two layers of sediment: one that is actually moving due to the fluid and one that is not moving but

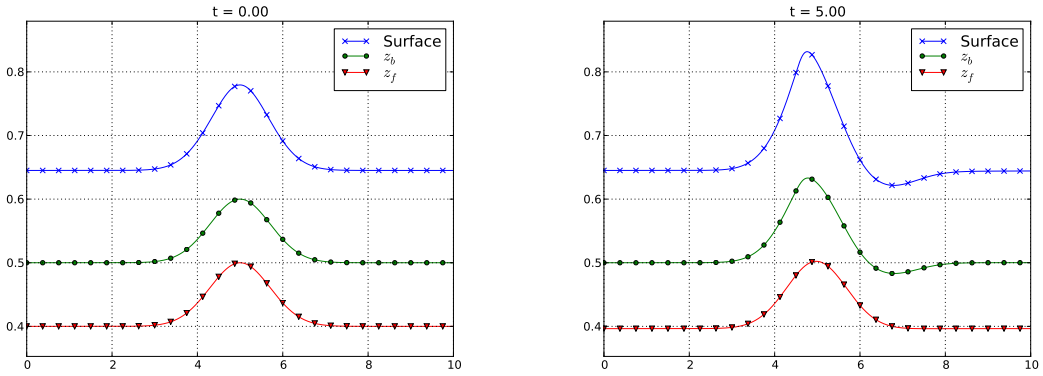

(a) Initial conditions

(b) Solution at $t = 5$

Figure 18: Free surface, bottom surface (z_b) and layer of sediments that are not moving (z_f) in a supercritical case for which there are three positive eigenvalues with the new bed load transport discharge

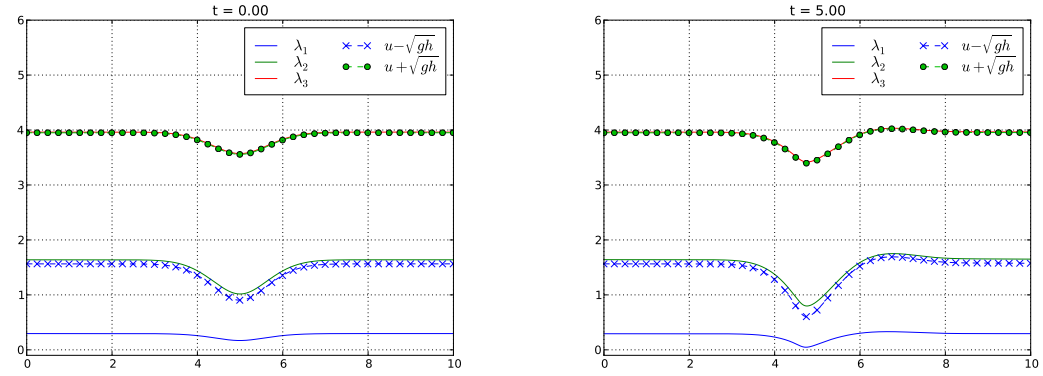

(a) Eigenvalues $t = 0$

(b) Solution at $t = 5$

Figure 19: Comparison between the eigenvalues of System (16) and the one of the Shallow-Water system in a supercritical case for which there are three positive eigenvalues with the new bed load transport discharge

could be entrained into the moving layer. As a consequence, the ideas taken into account are closer to the physics of the problem. Numerical simulations show that this generalization of solid transport flux is very promising. In particular, we remark that the vertical profiles on the front of an advancing dune (characteristic when using a classical formulation) are avoided and smoothed in a more realistic way.

Appendix A

Proof of Proposition 4.2

We define the two tangents of the curve $f(\lambda)$ which are parallel to $d(\lambda)$. Their intersections with $f(\lambda)$ are characterized by $f'(\lambda) = ghb$ which yields to two values of λ of the form

$$\lambda_\pm \overset{def}{=} \frac{2u + v_b \pm \sqrt{(u - v_b)^2 + 3(gh + ghb)}}{3}.$$

The two tangents are such that $d_\pm(\lambda_\pm) = f(\lambda_\pm)$. This implies the equations for the tangents are given by

$$d_\pm(\lambda) = ghb(\lambda - \alpha_\pm)$$

with

$$\alpha_\pm \overset{def}{=} \lambda_\pm - \frac{f(\lambda_\pm)}{ghb}. \tag{41}$$

The roots of $p_A(\lambda)$ which correspond to the eigenvalues of $A(W)$ are given as the intersection of $f(\lambda)$ and $d(\lambda)$ (see Figure 4).
Recall that $f(\lambda)$ is a third order polynomial with roots $\{\mu_1, \mu_2, \mu_3\} = \left\{v_b, u \pm \sqrt{gh}\right\}$. The equation $p_A(\lambda) = d(\lambda) - f(\lambda)$ will have 3 distinct solutions if and only if the line $d(\lambda)$ lies in between $d_-(\lambda)$ and $d_+(\lambda)$. This can be equivalently written as $\alpha_- < ku < \alpha_+$.
It can be checked that we always have $\alpha_- < u - \sqrt{gh} < u < u + \sqrt{gh} < \alpha_+$ so the system is always hyperbolic in the case $k = 1$. In the case $k = 7/6$, if $|u| < 6\sqrt{gh}$, we have $u - \sqrt{gh} < \frac{7}{6}u < u + \sqrt{gh}$ and thus the hyperbolicity condition is verified which concludes the proof.

□

Appendix B

Analytical solutions

Following [33], we can obtain analytical solutions for System (16). Considering the new solid transport discharge, a constant water discharge $q = hu$ and a water height that only depends on x (*i.e.* $h = h(x)$), then $u = u(x) = q/h(x)$, System (16) reduces to:

$$\begin{cases} q = cst, \\ \partial_t h = 0, \\ \partial_x \left(\dfrac{u^2}{2} + g\left(h + z_b\right) \right) = 0, \\ \partial_t z_b + \partial_x \widetilde{q}_b = 0, \\ \partial_t z_f = \dot{z}_d - \dot{z}_e. \end{cases} \tag{42}$$

Differentiating the third equation of System (42) with respect to time, we get: $\partial_{tx} z_b = 0$. Then, differentiating the fourth equation with respect to space, we obtain: $\partial_{xx} \widetilde{q}_b = 0$, and

$$\widetilde{q}_b = A(t)x + B(t) = z_m \alpha c Q \mathrm{sgn}(\tau_b)(\tau_b^*)^{m_1}(\tau_b^* - \tau_{cr}^*)_+^{m_2 - 1} = z_m C(\tau_b^*)^{m_1}(\tau_b^* - \tau_{cr}^*)_+^{m_2 - 1}.$$

In order to simplify the computations, we use Darcy-Weisbach friction law (in this case, S_f is a function of u only and does not depend on h) and we rewrite τ_b^* as :

$$\tau_b^* = \frac{f u^2}{8\left(\frac{\rho_s}{\rho} - 1\right) g d_s} = C_1 u^2.$$

Let us assume that $m_1 = 0$, $\tau_{cr}^* = 0$; then

$$\widetilde{q}_b = A(t)x + B(t) = z_m C (C_1 u^2)^{m_2 - 1}.$$

As $(C_1 u^2)^{m_2-1}$ does not depend on the time, we have:

$$0 = \partial_t \frac{A(t)x + B(t)}{z_m} = \frac{(A'(t)x + B'(t))z_m + (A(t)x + B(t))\partial_t z_m}{z_m^2},$$

and

$$\partial_t z_m = \frac{A'(t)x + B'(t)}{A(t)x + B(t)} z_m,$$

The last equation of System (42) reads:

$$\partial_t z_f = -\dot{z}_e + \dot{z}_d = -K_e \frac{V}{1-\varphi}(\tau_b^* - \tau_{cr}^*)_+ + K_d V \frac{z_m}{d_s} = -K_e \frac{V}{1-\varphi} C_1 u^2 + K_d V \frac{z_m}{d_s}$$

then

$$-A(t) = -\partial_x \widetilde{q}_b = \partial_t z_b = \partial_t (z_f + z_m) = -K_e \frac{V}{1-\varphi} C_1 u^2 + K_d V \frac{z_m}{d_s} + \frac{A'(t)x + B'(t)}{A(t)x + B(t)} z_m.$$

If we choose $A(t) = A$ and $B(t) = B$ two constants, then z_m does not depend on time and we obtain:

$$\begin{cases} -A = -K_e \dfrac{V}{1-\varphi} C_1 u^2 + K_d V \dfrac{z_m}{d_s}, \\ Ax + B = z_m C (C_1 u^2)^{m_2 - 1}, \end{cases}$$

that is

$$\begin{cases} K_e \dfrac{V}{1-\varphi} C_1 u^2 = A + K_d V \dfrac{z_m}{d_s}, \\ Ax + B = z_m C (C_1 u^2)^{m_2 - 1}, \end{cases} \quad \text{or} \quad \begin{cases} C_1 u^2 = \left(A + K_d V \dfrac{z_m}{d_s} \right) \dfrac{1-\varphi}{V K_e}, \\ Ax + B = z_m C \left(\left(A + K_d V \dfrac{z_m}{d_s} \right) \dfrac{1-\varphi}{V K_e} \right)^{m_2 - 1}. \end{cases}$$

Let us summarize the formulae: at the initial time,

$$\begin{cases} q = cst, \\ z_m \text{ is the solution of } Ax + B = z_m C \left(\left(A + K_d V \dfrac{z_m}{d_s} \right) \dfrac{1-\varphi}{V K_e} \right)^{m_2 - 1}, \\ u = \sqrt{\left(A + K_d V \dfrac{z_m}{d_s} \right) \dfrac{1-\varphi}{V K_e} \dfrac{1}{C_1}}, \\ h = \dfrac{q}{u}, \\ \partial_t z_b = -A \text{ with } z_{b|t=0} \text{ given by } \left(\dfrac{u^2}{2} + g\,(h + z_b) \right)_{|t=0} = cst, \end{cases} \tag{43}$$

and the evolution in time is performed as

$$z_f = -At + z_{f\,|t=0} = -At + z_{b|t=0} - z_m. \tag{44}$$

Acknowledgments

This research has been partially supported by the Spanish Government and FEDER through the Research project MTM2012-38383-C02-02, by the Andalusian Government through the project P11-RNM7069 and by the French CNRS via GdR EGRIN. E.D. F-N would likes to thank the MAPMO for the invitation of one month in the University of Orléans. The authors would like to thank Pierre-Yves Lagrée for the fruitful discussions. The numerical computations have been performed at the Laboratory of Numerical Methods of the University of Málaga.

References

[1] D. Simons, F. Şentürk, Sediment Transport Technology: Water and Sediment Dynamics, Water Resources Publ., 1992.

[2] K. Wilson, Bed-load transport at high shear stress, Journal of the Hydraulics Division 92 (1966) 49–59.

[3] J. Fredsøe, R. Deigaard, Mechanics of Coastal Sediment Transport, World Scientific Publishing Company, 1992.

[4] F. Exner, Über die wechselwirkung zwischen wasser und geschiebe in flüssen, Sitzungsber., Akad. Wissenschaften pt. IIa (1925) Bd. 134.

[5] M. Castro Díaz, E. Fernández-Nieto, A. Ferreiro, Sediment transport models in shallow water equations and numerical approach by high order finite volume methods, Computers & Fluids 37 (2008) 299–316.

[6] A. M. Ferreiro, Development of post-process technics of hydrodynamics flux, modelization of sediment transport problems and numerical simulation through finite volume technics, Ph.D. thesis, University of Sevilla, 2006.

[7] C. Savary, Transcritical transient flow over mobile beds, boundary conditions treatment in a two-layer shallow-water model, Ph.D. thesis, Louvain, 2007.

[8] B. Toumbou, D. Le Roux, A. Sene, An existence theorem for a 2-d coupled sedimentation shallow-water model, C. R. Math. Acad. Sci. Paris 344 (2007) 443–446.

[9] A. Grass, Sediment transport by waves and currents, SERC London Cent. Mar. Technol Report No. FL29 (1981).

[10] E. Meyer-Peter, R. Müller, Formulas for bed-load transport, in: 2nd meeting IAHSR, Stockholm, Sweden, pp. 1–26, 1948.

[11] L. Van Rijn, Sediment transport part 1: bed load transport., Journal of Hydraulic Engineering - ASCE 110 (1984) 1431–1456.

[12] P. Nielsen, Coastal Bottom Boundary Layers and Sediment Transport, World Scientific Pub Co Inc, 1992.

[13] A. Shields, Anwendung der Ähnlichkeitsmechanik und der Turbulenzforschung auf die Geschiebebewegung, Technical Report 26, Mitteilungen der Preussischen Versuchsanstalt für Wasserbau und Schiffbau, 1936.

[14] F. Charru, H. Mouilleron, O. Eiff, Erosion and deposition of particles on a bed sheared by a viscous flow, Journal of Fluid Mechanics 519 (2004) 55–80.

[15] R. Fernandez-Luque, R. van Beek, Erosion and transport of bedload sediment, J. Hydraul. Res. 14 (1976) 127–144.

[16] G. Sauermann, K. Kroy, H. J. Herrmann, Continuum saltation model for sand dunes, Physical Review E 6403 (2001) 031305.

[17] K. K. J. Kouakou, P.-Y. Lagrée, Evolution of a model dune in a shear flow, European Journal of Mechanics - B/Fluids 25 (2006) 348–359.

[18] A. Valance, V. Langlois, Ripple formation over a sand bed submitted to a laminar shear flow, Eur. Phys. J. B 43 (2005) 283–294.

[19] A. C. Fowler, N. Kopteva, C. Oakley, The formation of river channels, SIAM Journal on Applied Mathematics 67 (2007) 1016–1040.

[20] R. Slingerland, J. Harbaugh, K. Furlong, Simulating Clastic Sedimentary Basins: Physical Fundamentals and Computer Programs for Creating Dynamic Systems, Sedimentary Geology Series, PTR Prentice Hall, 1994.

[21] T. Morales de Luna, M. J. Castro Díaz, C. Parés Madroñal, A duality method for sediment transport based on a modified Meyer-Peter & Müller model, Journal of Scientific Computing 48 (2011) 258–273.

[22] F. Charru, Selection of the ripple length on a granular bed sheared by a liquid flow, Physics of Fluids 18 (2006) 121508.

[23] F. Charru, E. J. Hintch, Ripple formation on a particle bed sheared by a viscous liquid. part 1. steady flow, Journal of Fluid Mechanics 550 (2006) 111–121.

[24] H. A. Einstein, R. B. Krone, Experiments to determine modes of cohesive sediment transport in salt water, J. Geophys. Res. 67 (1962) 1451–1461.

[25] R. Bagnold, The Flow of Cohesionless Grains in Fluids, Royal Society of London Philosophical transactions. Series A. Mathematical and physical sciences, no. 964, Royal Society of London, 1956.

[26] B. Andreotti, P. Claudin, S. Douady, Selection of dune shapes and velocities. Part 2: A two-dimensional modelling, The European Physical Journal B 28 (2002) 341–352.

[27] B. Andreotti, P. Claudin, P. O., Measurements of the aeolian sand transport saturation length, Geomorphology 123 (2010) 343–348.

[28] E. Godlewski, P.-A. Raviart, Numerical approximation of hyperbolic systems of conservation laws, volume 118 of *Applied Mathematical Sciences*, Springer-Verlag, New York, 1996.

[29] S. Cordier, M. Le, T. Morales de Luna, Bedload transport in shallow water models: Why splitting (may) fail, how hyperbolicity (can) help, Advances in Water Resources 34 (2011) 980–989.

[30] I. Toumi, A weak formulation of roe's approximate riemann solver, J. Comput. Phys. 102 (1992) 360–373.

[31] M. Castro, J. Macías, C. Parés, A q-scheme for a class of systems of coupled conservation laws with source term. application to a two-layer 1-d shallow water system, M2AN Math. Model. Numer. Anal. 35 (2001) 107–127.

[32] C. Parés, M. Castro, On the well-balance property of roe's method for nonconservative hyperbolic systems. applications to shallow-water systems, M2AN Math. Model. Numer. Anal. 38 (2004) 821–852.

[33] C. Berthon, S. Cordier, O. Delestre, M.-H. Le, An analytical solution of the shallow water system coupled to the exner equation, Comptes Rendus Mathématique 350 (2012) 183–186.